pH-dependent reactive transport of uranium(VI) in unsaturated sand

ARTICLE *in* JOURNAL OF SOILS AND SEDIMENTS · MARCH 2015

Impact Factor: 2.14 · DOI: 10.1007/s11368-014-1018-x

4 AUTHORS, INCLUDING:

Burcu Uyusur

TUBITAK Marmara Research Center

12 PUBLICATIONS **22** CITATIONS

SEE PROFILE

Chunyan Li

Clemson University

5 PUBLICATIONS **5** CITATIONS

SEE PROFILE

Philippe Baveye

Rensselaer Polytechnic Institute

210 PUBLICATIONS **4,160** CITATIONS

SEE PROFILE

J Soils Sediments
DOI 10.1007/s11368-014-1018-x

SOILS, SEC 4 • ECOTOXICOLOGY • RESEARCH ARTICLE

pH-dependent reactive transport of uranium(VI) in unsaturated sand

Burcu Uyuşur · Chunyan Li · Philippe C. Baveye · Christophe J. G. Darnault

Received: 19 May 2014 / Accepted: 31 October 2014

Abstract
Purpose Uranium contamination of subsurface environments was once thought to be an isolated occurrence, mostly at production sites. But recent evidence has shown that the presence of uranium in phosphate fertilizers has caused massive amounts of this element to be released worldwide. Concerns are related to uranium movement to groundwater supplies and its significant toxicological risks to human populations. Information is direly needed on how geochemical processes control uranium transport in the vadose zone.
Materials and methods Laboratory experiments were performed to investigate the effects of the pH of the soil solution on the reactive transport of uranium(VI) in the vadose zone. The uranium solution was prepared by dilution of a 10^{-3} M stock solution of uranium perchlorate, ($UO_2(ClO_4)_2$), with DI water. Two U(VI) solutions were prepared at concentrations of 2×10^{-6} M at pH 6 and 11 and were percolated under steady-state conditions through columns filled with sand. The convective-dispersion equation (CDE) was used to analyze the tracer and uranium breakthrough curves resulting from the column experiments. The program CXTFIT was used to estimate the transport parameters of equilibrium and nonequilibrium (i.e., two-site and mobile-immobile) models applied to the experimental data.
Results and discussion Comparison of U(VI) breakthrough behavior at pH 6 with that of a nonreactive tracer indicated that U(VI) transport was significantly retarded, and about 52 % of the added U(VI) adsorbed to the quartz sand, likely in the cationic forms UO_2OH^+ and UO_2^{2+}. The adsorption was reversible upon the addition of deionized water. At pH 11, the U(VI) breakthrough curve increased gradually and reached a plateau value C/C_0 oscillating between 72 and 82 %. Upon reaction, Si was released from the dissolution of quartz sand, which allowed the possible transport of U(VI) following precipitation of a U(VI) containing solid, such as uranyl-silicate minerals, or sorption of U(VI) onto silica colloids. Two-site and mobile-immobile (MIM) models suggested an influence of either rate-limited mass transfer processes or immobile/mobile water partitioning in U(VI) reactive transport.
Conclusions The reactive transport of U(VI) governed by adsorption-desorption processes, precipitation, and complexation reactions in which kinetic behaviors are controlled by pH, solution chemistry, and heterogeneous flow regime impacts the mobility of U(VI). The column transport experiments indicated that under geochemical conditions and vadoze zone processes (preferential flow) that favor the mobility of U(VI), dissolved- and colloidal-phase associations of U(VI) may be transported rapidly and in high concentrations from the soil surface to the groundwater.

Keywords Geochemistry · Precipitation · Sorption · Two-site and mobile-immobile transport models · Uranyl silicates · Vadose zone

Responsible Editor: Dong-Mei Zhou

B. Uyuşur
Tübitak Marmara Research Center, P.K. 21 41470 Gebze, Kocaeli, Turkey

C. Li · C. J. G. Darnault (✉)
Department of Environmental Engineering and Earth Sciences, L.G. Rich Environmental Laboratory, Clemson University, 342 Computer Court, Anderson, SC 29625, USA
e-mail: cdarnau@clemson.edu

P. C. Baveye
Laboratory of Soil and Water Engineering, Department of Civil and Environmental Engineering, Rensselaer Polytechnic University, 319 Materials Research Center, 110 Eighth St., Troy, NY 12180, USA

Published online: 20 November 2014

1 Introduction

In various parts of the world, uranium produced by milling, mining, and isotopic enrichment operations has been released in the environment at concentrations that are causing significant societal concern (Abdelouas et al. 1998). The contamination of the Hanford Site, WA, is a prototypical example in this respect (Qafoku et al. 2004; Rod et al. 2010; Um et al. 2010a). High alkaline waste solutions leaked from underground tanks from the late 1950s through the 1960s, releasing more than 7 tons of uranium to the subsurface in an alkaline milieu (Jones et al. 2001). The Nevada Test Site (NTS) is another example, where approximately 600 underground nuclear tests have been conducted above the water table, releasing large quantities of uranium (Tompson et al. 2006). These cases, and similar ones in other geographical areas (Larson and Stone 2011; Mihalik et al. 2011), are examples of local ("point") sources of contamination that until recently attracted most of the attention of the media. However, some of the most worrisome accounts of uranium contamination are associated with a very different origin. Widespread, diffuse sources of pollution are related to the fact that uranium is a common constituent of phosphate fertilizers applied to agricultural soils. A recent estimate in Germany, for example, posits that fertilizer application there from 1951 to 2011 has led to the cumulative release of about 14,000 tons of uranium on agricultural land (Schnug and Lottermoser 2013).

In all of these situations, aside from possible toxicological effects related to exposure of microorganisms to dissolved uranium (e.g., Leduc et al. 1997), or of animals and humans to uranium-containing dust, key concerns revolve around the possibility for some of the uranium present in the vadose zone of soils (i.e., the water-unsaturated region of the subsurface) to percolate to the water table and contaminate groundwater supplies. Several processes are known to influence this downward transport of uranium. They have been studied extensively over the last two decades. Because uranium(IV) is only sparingly soluble in typical subsurface conditions and often precipitates as uraninite (UO_2), much of the information that is available on processes controlling the mobility of uranium relates to the other dominant form present in soil, uranium(VI). Uranium with this valence state occurs in the vadose zone and in groundwater in various dissolved species, in particular the relatively mobile uranyl cation (UO_2^{2+}) (McKinley et al. 2007a). Transport of uranium in the subsurface environment is impacted by the physicochemical properties of the porous media, the characteristics of the solution chemistry, the presence of complexing ligands, and "hydrologic history" (Um et al. 2010b; Miller et al. 2013a, b; Lesher et al. 2013). In particular, the transport of uranium is controlled by the surface properties of the porous media, the presence of microfractures within the particles constitutive of the porous media, the physical and chemical heterogeneity of the porous media materials, and the degree of saturation of the porous media (Catalano et al. 2006; Arai et al. 2007; Stubbs et al. 2009; Rod et al. 2012; Miller et al. 2013a, b). The release of uranium from microfractures and the transport of uranium in unsaturated porous media were both found to be governed by diffusion-limited kinetics (Liu et al. 2004, 2006; Rod et al. 2012). The wetting and drainage phenomena occurring in the unsaturated zone due to surface and subsurface water interactions have been simulated to investigate the effects of water table fluctuation and capillary fringe formation and dynamics on the release rate of uranium with time and the controlling chemical processes (Qafoku et al. 2005; Um et al. 2010b; Ma et al. 2014a, b). The change in hydrodynamics, the "hydrologic history" of the porous media, the duration of equilibration time, and the surface and subsurface water interactions impacted the dynamic of U(VI) release and transport behavior; as the time of equilibrium increased, release and transport of U(VI) increased, and geochemical processes such as dissolution and precipitation occurred due to ion exchange (Gabriel et al. 1998; Zheng and Wan 2005; McKinley et al. 2007a, b; Williams et al. 2007; Um et al. 2010b; Ma et al. 2014a, b; Shang et al. 2014). Complexing ligands, such as natural organic matters, may enhance U(VI) transport (Artinger et al. 2002; Mibus et al. 2007; Crançon et al. 2010; Lesher et al. 2013) and remobilization of previously adsorbed uranium (Lesher et al. 2013). Competition between soluble organic matters and adsorption sites for U(VI) is also known to impact the fate and transport of uranium (Lenhart and Honeyman 1999; Crançon and van der Lee 2003). Adsorption of U(VI) during transport in unsaturated porous media has been observed to be correlated with the presence of immobile water; therefore, the sorption and transport of U(VI) in unsaturated porous media are impacted by partition between mobile and immobile water (Gamerdinger et al. 2001a, b). "The fate of uranium in soil and subsurface environment may be consequently driven by a delicate balance of U(VI) association between immobile and mobile phases" (Crançon et al. 2010).

Adsorption is one of the key determinants of the mobility of U(VI) in the subsurface environment. Iron oxides, including ferrihydrite (Reich et al. 1998; Waite et al. 1994), goethite (Moyes et al. 2000; Redden et al. 2001), and hematite (e.g., Bargar et al. 2000), are known to strongly adsorb U(VI). Important geochemical parameters affecting uranium adsorption in the subsurface environment include pH and ionic strength of the soil solution, concentration of complexing ligands such as dissolved carbonates (Lesher et al. 2013), oxidation/reduction conditions, and mineralogy. Distribution coefficients for U adsorption with respect to pH were reported by the U.S. EPA (1999). Depending on the pH value, the amount of U that is adsorbed in carbonate solutions varies; U adsorption augments as the pH value increases from 3 to 7, and it diminishes when the pH value is above the threshold value of 7 (e.g., Andersson et al. 1982; Giblin 1980; Kaplan

and Serne 1995; Kaplan et al. 1998; Salter et al. 1981; Sheppard and Thibault 1988; Zachara et al. 1992). When there is no carbonate in the soil environment, "[Read et al. (1993) and Sims et al. (1996)] interpreted uranium adsorption as a surface complexation process of positively charged uranium species, e.g., UO_2OH^+ and UO_2^{2+}on negatively charged surface sites" (Abdelouas et al. 1998). The adsorption is also impacted by the amount of pH-dependent exchange sites located at the surface of minerals that are subject to changeable charges due to a variable soil solution chemistry. Arnold et al. (1998) show that the highest sorption of U(VI) on the mineral surfaces (muscovite, quartz, chlorite, and albite feldspar) occurred near pH 7. Similarly, Barnett et al. (2000) observe substantial sorption of U(VI) to heterogeneous, natural subsurface media, mostly "sand-sized quartz" containing Mn and Fe oxides, under pH conditions between 4.5 and 8.5.

Another important geochemical process impacting the mobility of uranium in subsurface environments is the precipitation of uranium-containing solids. Dissolution of "unstable primary minerals (e.g., feldspars and micas) and stable minerals (e.g., quartz, aluminosilicate clays and sesquioxides)" (Mashal et al. 2004) releases variable amounts of Si and Al, which may lead to secondary mineral precipitation (Serne et al. 2002; Mashal et al. 2004). Upon reacting with various ions in solution, U(VI) can precipitate as hydroxide (e.g., uranyl hydroxide, α-$UO_2(OH)_2$), silicate (e.g., boltwoodite, $K(H_3O)UO_2(SiO_4)\cdot nH_2O$), and phosphate (e.g., metatorbernite, $Cu(UO_2)_2(PO_4)_2\cdot 8(H_2O)$) phases, as well as coprecipitate with calcite. Analysis of samples taken from the Hanford Site has shown that fractured porous media allow the removal of uranyl from the subsurface solution by diffusion and precipitation and that when present in these fractures, dissolved silica causes supersaturation with respect to sodium boltwoodite ($Na(UO_2)(SiO_3OH)\cdot 1.5H_2O$) and/or uranophane ($Ca(UO_2)_2(SiO_3OH)_2(H_2O)_5$) (Liu et al. 2004; McKinley et al. 2007b; Wang et al. 2005). The uranyl-silicate precipitates seem to exist as discrete crystals in shallow soils and shallow depths, which, as soil solution conditions change, can lead to the sustained release of uranium through mineral dissolution (Um et al. 2009).

Besides adsorption and precipitation, colloidal or colloid-facilitated transports have also been recognized as important mechanisms controlling the migration of radioactive contaminants (Contardi et al. 2001; Chen and Flury 2005; Zhuang et al. 2003). The two possible scenarios for transport as colloids are the adsorption of U(VI) to colloidal particles in suspension in the soil water and the formation of U(VI) or U(IV) colloids. For the first case, U(VI) may unalterably adsorb to soilborne colloids such as clay (Missana et al. 2004) or iron-containing secondary minerals (Zänker et al. 2006), which then become mobilized. In the second scenario, the formation of U(IV) or U(VI) colloids can materialize under oxidizing or reducing conditions, respectively. Mertz et al. (2003) examined the colloidal properties of two uranium minerals, uranium dioxide (UO_{2+x}) with U in the +4 oxidation state and metaschoepite ($UO_3n(H_2O)$ with U in the +6 oxidation state. Fortner et al. (2002) characterized colloids that were generated in a set of aqueous corrosion experiments with irradiated and nonirradiated metallic uranium fuel. They observed that stable suspensions of small (1–10 nm diameter) spherical uranium oxides (UO_2) were generated and aggregated to approximately 100–200 nm colloids. Large acicular uranium silicate colloids were also detected in small numbers in silicate solutions.

This brief overview of the literature shows that a number of possibly competing physicochemical processes can in principle affect the fate of uranium in subsurface environments, subject to several factors, like the pH and ionic strength of the aqueous phase, which can itself be moving at variable speeds in any given time frame. In recent years, the effect of these different parameters has been analyzed in some detail in the case of water-saturated sediments, i.e., in aquifers or in the capillary fringe (Miller et al. 2013a, b; Um et al. 2010b; Wellman et al. 2008; Yin et al. 2011), and progress continues to be made. By comparison, there is a dearth of information about the fate and transport of uranium in water-unsaturated soils, i.e., in the vadose zone. Ku et al. (2009) present a first attempt at the development of a model simulating the transport of uranium in the vadose zone, associated with the nonsteady state and discontinuous movement of the liquid phase. The model constraints for simulating uranium transport are its ability to simulate sink terms and surface-water interactions. The model predicts that the discontinuous flow that takes place in the vadose zone induced an interdependence among "reciprocal U concentration and $^{234}U/^{238}U$ ratio" in the vadose zone leachate, allowing for characterization of "rates of dissolution and [alpha]-recoil of U isotopes" (Ku et al. 2009). These predictions appear borne out by circumstantial evidence at a site (Peña Blanca) in Mexico (Ku et al. 2009), but other than that, there are no direct experimental observations related to uranium transport in unsaturated soils, which could be used to assess the suitability of model efforts. To predict the potential risks to groundwater resources in various parts of the world, experimental information is direly needed in particular on the effects of geochemical processes on the transport and retention of uranium(VI) through the vadose zone in near-neutral and alkaline (corrosive/caustic) conditions, as well as the interaction of U(VI) with secondary minerals resulting from weathered sediments under corrosive/caustic conditions.

In this context, the objectives of the research described in this article were to experimentally investigate the mobility of U(VI) and to model its transport mathematically, through the vadose zone under different pH conditions. To achieve these objectives, we conducted scoping experiments to (1) characterize the transport and retention of U(VI) in unsaturated quartz sand columns at pH 6 and pH 11, (2) establish the

effects of pH on the release and remobilization of U(VI) from the quartz sand columns by switching the initial geochemical solution conditions from U(VI) at pH 6 and pH 11 to deionized water, and (3) model the reactive transport of U(VI) in unsaturated porous media under different pH conditions using the convection-dispersion equation (CDE).

2 Theory

The CDE for one-dimensional transport of reactive solutes may be written as (Parker and van Genuchten 1984):

$$R\frac{\partial c_r}{\partial t} = D\frac{\partial^2 c_r}{\partial x^2} - v\frac{\partial c_r}{\partial x} - \mu c_r + \gamma(x) \quad (1)$$

where c_r is the resident concentration of the liquid phase (ML^{-3}), v is the average pore-water velocity (LT^{-1}), R is the retardation factor, D is the dispersion coefficient (L^2T^{-1}), μ is a first-order rate coefficient, $\gamma(x)$ is a zero-order rate coefficient, x is the distance from the inlet (L), and t is the time (T). Analytical solutions of this CDE for a range of initial and boundary conditions are provided by Parker and van Genuchten (1984).

The transport of reactive solutes in porous media may also be impacted by physicochemical nonequilibrium processes (Nielsen et al. 1986; Aharoni and Spark 1991). Chemical nonequilibrium processes may arise from adsorption kinetics. The kinetics of adsorption of solutes in porous media may include the adsorption of solutes on two different sites, each of them governed by different adsorption kinetics—for example by instantaneous adsorption on one type of site and by first-order kinetics on the other type of site (Selim et al. 1976; Cameron and Klute 1977). A physical nonequilibrium process may be induced by heterogeneous flow regime that can be simulated by two regions—a mobile water region and an immobile water region (Coats and Smith 1964; van Genuchten and Wierenga 1976). The mass transfer between the mobile and immobile water regions can be simulated using first-order kinetics. A single dimensionless form of the CDE can be used to represent both the two-site and the mobile-immobile (MIM) models with linear adsorption kinetics and steady-state flow conditions (Nkedi-Kizza et al. 1984; van Genuchten and Wagenet 1989).

The dimensionless form of the CDE for two-site and MIM models may be written as (Nkedi-Kizza et al. 1984):

$$\beta R\frac{\partial C_1}{\partial T} = \frac{1}{P}\frac{\partial^2 C_1}{\partial Z^2} - \frac{\partial C_1}{\partial Z} - \omega(C_1 - C_2) - \mu_1 C_1 + \gamma_1(Z) \quad (2)$$

$$(1-\beta)R\frac{\partial C_2}{\partial T} = \omega(C_1 - C_2) - \mu_2 C_2 + \gamma_2(Z) \quad (3)$$

where the subscripts 1 and 2 represent equilibrium and nonequilibrium sites, respectively, β is a partitioning coefficient, and ω is a dimensionless mass transfer coefficient. The definitions of the dimensionless parameters for one-site and two-site adsorption models and a two-region model are given in Toride et al. (1999), along with analytical solutions to the dimensionless CDE.

3 Materials and methods

3.1 Sand material and preparation of uranium spiking solutions

Uranium transport experiments were conducted on chemically treated ASTM 20/30 mesh (0.591–0.841 mm) Ottawa Silica Sand purchased from the U.S. Silica Company. Before use in the experiments, the sand was chemically treated with concentrated sulfuric acid, H_2SO_4 (Fisher Scientific), in an effort to condition the surface and remove iron oxide coatings. The chemically treated sand was then rinsed with deionized (DI) water and placed for 2 days, at 75 °C, in DI water that was changed every day. Finally, the sand was rinsed at least ten times and dried in an oven (105 °C, 24 h), following Bickmore et al. (2001).

The uranium solution prepared for the column experiments consisted of U(VI) at a concentration of 2×10^{-6} M. The uranium solution was prepared by the dilution of a 10^{-3} M stock solution of uranium perchlorate ($UO_2(ClO_4)$) with DI water. The simple dilution produced a U(VI) solution at pH 6, which did not require further pH adjustment. The U(VI) solution at pH 11 was obtained by adjustment using 10 M NaOH. Sodium perchlorate was added to each uranium solution at a concentration of 1 mM, as perchlorate ions were used as a nonreactive tracer.

3.2 Experimental setup

Unsaturated flow and transport experiments were carried out in vertical plastic columns (3.8 cm inside diameter and 25 cm long) at room temperature. In an effort to prevent layering, columns were packed by adding approximately 1 cm increments of dry quartz sand, tamping the sand in the column, and then briefly vibrating the column. Rainfall simulation was performed by dispersing the influent solution at several points distributed uniformly at the sand surface. A 10 μm Teflon® filter (Omnipore™ Millipore®) was placed at the top and the bottom of the column. The filter located at the top of the

column contributed to disperse the incoming liquid. Influent solutions were delivered to the column using a MasterFlex peristaltic pump (Cole-Parmer Instrument Company). Column effluent samples were collected from the bottom of the column as 9 mL fractions.

3.3 Column experiments

Column experiments were conducted to investigate the transport and retention of uranium in unsaturated porous media at pH 6 and pH 11 and to determine the extent of the possible release and re-entrainment of uranium from quartz sand following ionic strength changes in the geochemical solution. Column experiments included three phases. The first phase consisted of injection of DI water to the top of the column to simulate rainfall until a steady-state flow was reached in the column. The steadiness of the flow was attained when the outflow rate became equal to the inflow rate, as determined by measuring the outflow at frequent intervals. The amounts of water in the column inflow and outflow were measured, and their differences were used to compute the degree of saturation of the porous media. The second phase was the injection of the 2×10^{-6} M U(VI) spiking solutions at pH 6 and pH 11, containing the nonreactive tracer sodium perchlorate. The amount of the spiking solutions introduced into the columns corresponded to eight times the volume of water present in the unsaturated columns at steady state. The third phase (elution phase) involved switching from the injection of the spiking U(VI)-tracer solution to the injection of DI water to introduce a change in ionic strength and pH in the geochemical solution. The hydraulic properties of the experimental columns at pH 6 and pH 11 are presented in Table 1. The pore flow velocities were 1.14 and 2.5 cm/min at pH 6 and pH 11, respectively.

3.4 Analytical methods

The effluent samples were analyzed for uranium and silica using an inductively coupled plasma optical emission spectrophotometer (ICP-OES) (Perkin Elmer, Optima 4300 DV). Calibration curves were established, covering a silica concentration range from 0.05 to 20 ppm and a uranium concentration range from 0.05 to 10 ppm. The concentration of the perchlorate tracer was measured using ion chromatography (IC) (Dionex, Ion Chromatography System (ICS) 2500).

3.5 Mass balance and speciation calculations

Dimensionless breakthrough curves (BTCs) of uranium were determined by plotting the value of the normalized concentration to the initial concentration versus the cumulative volume eluted from the column. The area below the U(VI) BTC of the adsorption front (until the elution phase) was numerically integrated to assess the percentage of uranium retained in the column.

All speciation modeling calculations were carried out with The Geochemist's Workbench® 4.0.3 (GWB) (Bethke 2002). The P_{CO2} was assumed to be in equilibrium with the atmosphere ($\sim3\times10^{-4}$ kPa). Dissolved Si derived from quartz dissolution was calculated according to a simple first-order kinetic rate law. For the pH 6 experiment, the dissolution rate constant of quartz and specific surface area value were taken from Rimstidt and Barnes (1980) as 4.2×10^{-18} mol/cm^2 s and 910 cm^2/g, respectively. The specific surface area was assumed to be similar to that of Rimstidt and Barnes (1980) because the grain size in the two sets of experiments was similar. For the pH 11 experiment, the dissolution rate constant was taken from Bickmore et al. (2006) by linear regression of the reaction rate constants at pH 11 determined from 59 to 80 °C and by extrapolation to room temperature.

3.6 Modeling

The dimensionless CDE was used to analyze the tracer and uranium data from breakthrough curves that depict the dimensionless effluent concentration C/C_0 as a function of cumulative pore volumes eluted, resulting from the column transport experiments. The program CXTFIT, developed by Parker and van Genuchten (1984), was used to fit the parameters of the equilibrium and nonequilibrium (i.e., two-site and MIM) models. We used the CXTFIT code version that has been implemented in Excel by Tang et al. (2010) and is available from Oak Ridge National Laboratory (ORNL) (CXTFIT/EXCEL 2013).

To model the transport of the tracer and reactive solute (i.e., uranium) using equilibrium and nonequilibrium (two-site and MIM) models, we first enter the input parameters L and v, and then the estimated parameters (θ/θ_m, T_0, R, λ, η, f, α) are optimized to best fit the simulated reactive transport models to the experimental data. Finally, the P, β, and ω parameters

Table 1 Hydraulic properties of the columns

Experiment	Flow rate (mL/min)	Pore velocity (cm/min)	Residence time (min)	Porosity	Column water volume (mL)	Degree of saturation (%)	Bulk density (g/cm^3)
pH 6	2.8	1.14	22	0.46	38.9	30	1.44
pH 11	2.8	2.5	10	0.46	26	23.8	1.44

corresponding to the simulated reactive transport models and the resulting SSR, RMSE, and R^2 values of the predictive models are computed as output parameters by CXTFIT/EXCEL.

4 Results and discussion

4.1 Speciation of uranium

The computed U(VI) aqueous speciation in the pH 6 influent and effluent solutions (Table 2) is dominated by two positively charged complexes, UO_2OH^+ and UO_2^{2+}, and two neutral species, $UO_2(OH)_2$(aq) and UO_2CO_3(aq). No minerals are supersaturated in any solution at pH 6. At pH 11, the influent and effluent solutions are also not supersaturated with respect to any minerals, and the primary aqueous U(VI) species is $UO_2(CO_3)_3^{4-}$

4.2 Effects of pH on uranium transport

The BTC of the nonreactive tracer perchlorate in the experiment at pH 6 is characterized by a fast rising phase shortly after the introduction of the influent solution, reaching a plateau value C/C_0 of 98–99 %, followed by a declining phase as the elution phase with DI water begins. Relative to this tracer BTC, the breakthrough time of U(VI) is slightly delayed. The discrepancy between the tracer and U(VI) BTCs and the subsequent gradual increase in the concentration of U(VI) in the effluent to reach a plateau value C/C_0 of 1 indicate that U(VI) is significantly retarded during its transport through the chemically treated sand, compared to the transport of the nonreactive tracer. This retardation can be accounted for by nonlinear interactions between U(VI) and quartz sand surfaces. Other studies have also demonstrated similar sorption and transport behavior of U(VI) (Prikryl et al. 2001; Phillippi et al. 2007; Ma et al. 2010). Under unsaturated conditions, uranyl ion is thought to be "complexed by negative fixed-charge or amphoteric sites on mineral surfaces" (McKinley et al. 2007a). Complexation reactions in the soil solution are up against uranium to interact with surfaces; this competition for access to sites may also impact the degree of the sorption reaction (McKinley et al. 2007a). At pH 6, there are no significant competing ions, and so the retardation of U(VI) in the column is probably due to adsorption of the dominant cationic species including UO_2OH^+ and UO_2^{2+} / (Table 2). Quartz sand has an isoelectric point at pH 2.44 because of the amphoteric character of its silanol groups (Jada et al. 2006) and, therefore, a net negative surface charge ($\equiv SiO^-$) at pH 6. Consequently, the positively charged U(VI) could bind to the negatively charged silanol sites.

In order to evaluate the sorbed fraction of U(VI), the area below the U(VI) BTC of the adsorption front (until the elution phase) is numerically integrated. This value is then subtracted from the total amount of U(VI) input in order to find the amount of U(VI) sorbed onto the quartz sand. This calculation yields approximately 0.53 μg of U(VI) per gram of sand, corresponding to 52 % of the total input of U(VI). This quantity is compared with the total number of sorption sites on quartz surfaces in the column to confirm whether or not adsorption is the process most likely to have caused the retardation of U(VI) transport. The specific surface area and the surface sites present are taken from the literature as 910 cm^2/g (Rimstidt and Barnes 1980) and 4.81 sites/nm^2 (Arnold et al. 2001), respectively. The estimated total number of sites on the quartz is thus 5.4×10^{19} in the column, which is much larger than the number (1.64×10^{17}) of U(VI) atoms removed in the column. This suggests that adsorption may be a plausible explanation for the retardation. These results are comparable to results from published analogous batch and column studies. In their investigation using batch experiments, Fox et al. (2006) demonstrated that U(VI) sorption declined from about 90 % at pH 7 to almost 0 % at pH 8.75 (U(VI) influent concentration=10^{-6} M; quartz=25 g/L; ionic strength=5 and 32 mM; specific surface area of quartz=0.32 m^2/g). The results of their surface complexation model were in good agreement with their data. Although silica dissolved into the solution, sorption was not affected by the dissolved silicate concentration. Arnold et al. (2001) measured 50 % sorption of U(VI) in batch studies at pH=6.5 (U(VI) influent concentration=1×10^{-6} M; ionic strength=0.1 M $NaClO_4$; specific surface area of quartz=0.2 m^2/g). Mibus et al. (2007) found 43 % recovery of U(VI) in a saturated quartz column study at pH=7.5 (pulse input ~3.7 pore volumes; U(VI) influent concentration=1.1×10^{-5} M; ionic strength=0.1 M $NaClO_4$; specific surface area of quartz=0.03 m^2/g) and concluded that surface complexation is the reason for the retardation of U(VI) transport and that sorption processes are the rate-controlling step. Similar findings have been reported by US EPA (U.S. Environmental Protection

Table 2 Dominant U(VI) species in influent and effluent solution at pH 6 and 11

Aqueous species	Molality	mg/kg solution	γ^a	log a^b
pH 6				
$UO_2(OH)_2$(aq)	1.624×10^{-6}	0.4939	1.0000	−5.7893
UO_2OH^+	2.085×10^{-7}	0.05985	0.9973	−6.6820
UO_2^{2+}	3.388×10^{-8}	0.00915	0.9892	−7.4747
UO_2CO_3(aq)	3.353×10^{-8}	0.01107	1.0000	−7.4746
pH 11				
$UO_2(CO_3)_3^{4-}$	2×10^{-6}	0.4491	0.0001	−9.8994

[a] γ, activity coefficient

[b] log a, log [(Molality)×(activity coefficient)]

Agency) (1999): "this pH-dependent behavior is related to the pH-dependent surface charge properties of the soil minerals and complex aqueous speciation of dissolved U(VI), especially near and above neutral pH conditions where dissolved U(VI) forms strong anionic uranyl-carbonato complexes with dissolved carbonate." Smaller amounts of adsorbed uranyl are expected at the lower pH due to the surface charge of silica.

In the BTC of U(VI) at pH 6 (Fig. 1), the flushing of the unsaturated porous media with DI water results in a sharp increase in U concentration, leading to an observed U(VI) elution peak C/C_0 of 0.54. This elution peak is a clear indication of U(VI) desorption from the surface of quartz sand grains and U(VI) remobilization. The transport of U(VI) is affected by the U(VI) adsorption/desorption kinetics at the silica quartz grain/water interface (Cheng et al. 2007; Malin and Geiger 2010; Qafoku et al. 2005; Stoliker et al. 2011) that may result from "diffusion-limited surface complexation reactions" (Shang et al. 2011). The release of U(VI) adsorbed at the surface of quartz sand grains demonstrates the reversibility of the attachment processes of U(VI) under saturated conditions. Recent studies have also demonstrated that the desorption of U(VI) is controlled by many geochemical variables including pH, alkalinity, carbonate concentration, and mineral type (Handley-Sidhu et al. 2009; Liu et al. 2009; Miller et al. 2013b; Stoliker et al. 2013; Yabusaki et al. 2008, 2011; Yin et al. 2011). The release and remobilization of U(VI) due to reversible attachment as a result of a change in solution geochemistry has also been previously reported at low pH (Crançon et al. 2010; Gabriel et al. 1998; Ho and Miller 1986; Zheng and Wan 2005).

For the pH 11 experiment, the flow rate, influent U(VI) concentration, and other physical experimental conditions were the same as in the pH 6 experiment. The BTC of the nonreactive tracer curve at pH 11 (Fig. 2) is similar to the one at pH 6. However, at pH 11, the U(VI) species behave differently than the tracer and the U(VI) species at pH 6. After a slight delay compared with the tracer BTC, the U(VI) BTC starts to increase gradually to reach a plateau value C/C_0 oscillating between 72 and 82 %. As DI water is applied to flush the unsaturated porous media containing U(VI) and to initiate the elution phase, no U(VI) elution peak is observed in the U(VI) BTC. After switching to the DI water for the elution phase, the area under the desorption curve is integrated in an effort to determine any desorbed fraction of U(VI). The tracer and U(VI) curves are virtually coincidental, which implies that almost none of the U(VI) is leached upon elution. Therefore, there is no release or remobilization of U(VI) under this geochemical solution change.

The BTC of Si (Fig. 2) is characterized first by a sharp increase to almost C/C_0=0.9 (at the introduction of the pH 11 U(VI) solution). The concentration then decreases monotonically to 0.07–0.08 mM and remains relatively constant at this level. Upon flushing with DI water, the Si concentration again shows an increase from 0.07 to 0.4 mM for a short period of time, after which point the concentration again reaches another equilibrium value of 0.01 mM (Fig. 2). Visual observations confirm small amounts of precipitate at the bottom of some of the sealed effluent collection tubes months after the analyses. Consequently, the Si measured by ICP-OES is considered to be only part of the amount that actually exited the column. It is likely that when the analysis was performed, there was already a small amount of precipitate at the bottom of the tubes that went unnoticed and that the solutions were not well mixed upon injection into the instrument. The measured concentration of Si in the effluent (the part that did not precipitate) was higher than expected based on estimates from quartz dissolution, but lower than the concentration that would be in equilibrium with quartz. One possible explanation is the initial presence of a gel-like layer of Si when

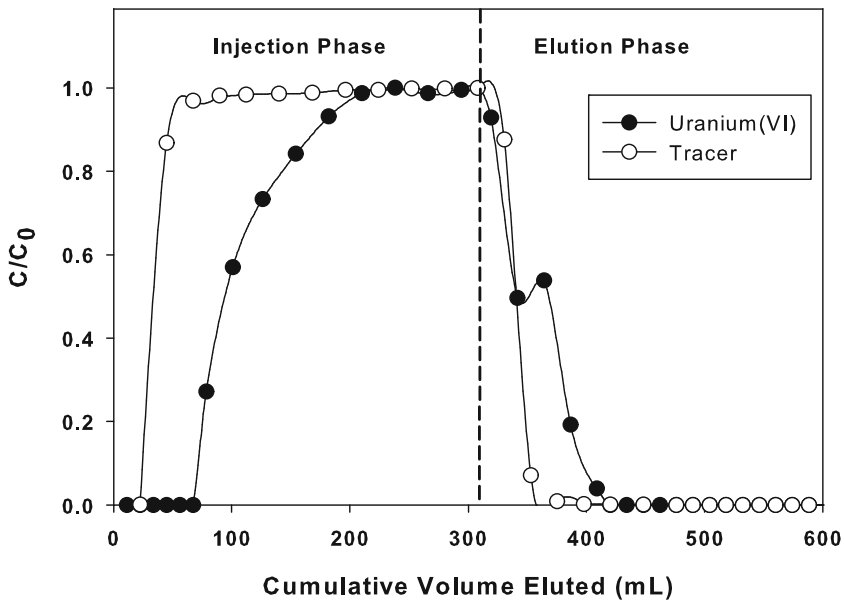

Fig. 1 Breakthrough curves of U(VI) and of a nonreactive tracer (sodium perchlorate) at pH 6 during injection and elution phases. The dimensionless effluent concentration C/C_0, where C and C_0 represent the effluent and influent concentrations, respectively, is plotted as a function of the cumulative volume eluted

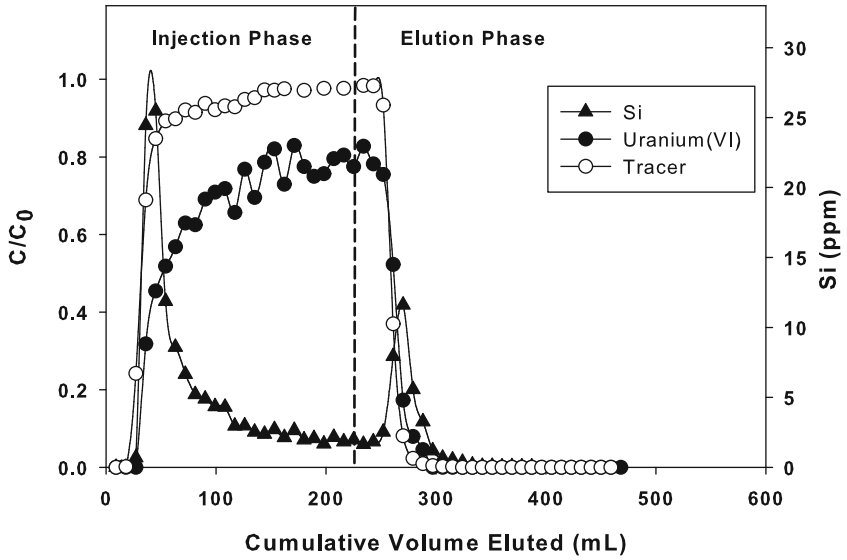

Fig. 2 Breakthrough curves of U(VI), silica, and a nonreactive tracer (sodium perchlorate) at pH 11 during injection and elution phases. The dimensionless effluent concentration C/C_0, where C and C_0 represent the effluent and influent concentrations, respectively, is plotted as a function of the cumulative volume eluted

quartz is placed in contact with water. Still, no general agreement has been established in the literature regarding the existence of a gel layer on quartz sand (Ball et al. 1997; Huber and Lützenkirchen 2009). Another explanation may be that when the surface of the quartz contacted the alkaline solution, higher amounts of silica were dissolved than anticipated. Si release from quartz sand has also been observed under highly alkaline solution (Wang and Um 2012). The third possibility is that the surface of the quartz still contained some amorphous structure despite the pretreatment with sulfuric acid to remove the more soluble amorphous.

We expect that uranium retardation in the quartz sand occurs either through sorption or precipitation. This decrease in U(VI) concentration at basic pH cannot result from sorption since the dominant U(VI) aqueous species under these conditions are anionic U(VI) carbonate complexes as shown by the aqueous speciation calculation. Consequently, a precipitation reaction is suspected. Visual observations showed a precipitate at the bottom of the plastic effluent collection tubes, but it is unknown if precipitation also occurred inside the column. The area below the BTC was integrated and subtracted from the total U(VI) input into the column. The results show that 34 % of the uranium is removed either in the column or is not analyzed in the effluent tubes because of coprecipitation with silica.

Two scenarios may be considered in this respect. The first is that the decrease of U(VI) concentration, as well as the changes in the concentrations of Si dissolution in the experiments, suggests the possibility of formation of a mineral precipitate phase in alkaline vadose zone water, as also reported by McKinley et al. (2006). Possible uranyl-silicate phases in our conditions are sodium boltwoodite $Na(UO_2)(SiO_3OH)\cdot 1.5H_2O$, soddyite $(UO_2)_2SiO_4\cdot 2(H_2O)$, and schoepite $(UO_2)_4O(OH)_6\cdot 6(H_2O)$. However, the GWB computation results show that no mineral was supersaturated at the end of the experiment nor at the point when the measured effluent Si concentration was the highest. The only U(VI) species was calculated to be $UO_2(CO_3)_{42}$. The reason for the failure of the model predictions could be related to uncertainties in the surface area and the dissolution rate constant of the initial quartz surface. On the effluent side, the solutions were not calculated to be supersaturated simply because a precipitate had already been formed and was inadvertently missed in the analysis. The precipitation of minerals at high pH values has been reported in some studies. An increase in Kd values has been noted at high pH, caused by the precipitation of U(VI) containing solids. For instance, Kaplan et al. (1998) established that U(VI) sorption was constant as UO_2^{2+} concentrations varied between 3.3 and 100 μg/L at pH 8.3 and an ionic strength of 0.02 M. After pH 8.3, the apparent Kd increased to 400 mL/g where U(VI) containing solids precipitated out. The one-dimensional transport code Xlt (Bethke 1996), run by Viani and Torretto (1998), simulated the precipitation of soddyite on a mixture of quartz and hematite column at pH 8 with an influent concentration of 2×10^{-6} M of U(VI) and assumed that quartz solubility controls the level of silica in solution.

A second possible scenario is that the dissolution of Si from the quartz surface could have caused the formation of silica colloids, which were then transported through the column. Having a high surface area, the silica colloids might have taken up some of the uranium from the infiltrating solution. Aggregation may have caused such colloids to stay in the column and/or settle out in the effluent tube. The sorption of uranium onto silica colloids has been observed to be an irreversible reaction (Lu et al. 2000; Zhuang et al. 2003). Since the sorption of U(VI) onto silica colloids decreases after ~pH 8 (Baik and Hahn 2001), the loss of U(VI) likely occurred by precipitation of a U(VI)- and Si-containing phase, which was at least partly mobilized under the unsaturated flow conditions. The coprecipitation of uranium with colloidal silica was postulated to occur via the incorporation of uranium as uranyl-silica-hydroxyl complexes (Zielinski 1980).

Table 3 Parameters for the equilibrium and nonequilibrium two-site and MIM CDE model simulations

		pH	L (cm)	v (cm day^{-1})	T_0	R	P	β	ω	λ	θ_m/θ	η	f	α	SSR	RMSE	R^2
Equilibrium CDE	Tracer	11	25	3750	2	–	–	–	–	800	–	–	–	–	1.0933	0.1743	0.8448
	Uranium (VI)	11	25	3750	1.75	–	–	–	–	45	–	–	–	–	0.7072	0.1402	0.8052
	Tracer	6	25	1641	2.6	–	–	–	–	500	–	–	–	–	0.7022	0.1530	0.8980
	Uranium (VI)	6	25	1641	1.77	–	–	–	–	1.75	–	–	–	–	0.2243	0.0789	0.9583
Nonequilibrium CDE two-site	Tracer	11	25	3750	1.77	1	37.879	0.25	0.053	0.66	0.25	–	0.25	10.5	0.0278	0.0321	0.9942
	Uranium (VI)	11	25	3750	1.7	2	15.06	0.25	0.344	1.66	0.25	–	0.11	31.5	0.1397	0.0719	0.9265
	Tracer	6	25	1641	2.4	1	37.879	0.25	0.011	0.66	0.25	–	0.25	1	0.0180	0.0258	0.9973
	Uranium (VI)	6	25	1641	2	3.2	15.06	0.25	0.018	1.66	0.25	–	0.25	0.5	0.0857	0.0563	0.9824
Nonequilibrium CDE MIM	Tracer	11	25	3750	1.77	–	37.879	0.25	0.053	0.66	0.25	0.025	–	–	0.0276	0.0308	0.9947
	Uranium (VI)	11	25	3750	1.7	2	15.06	0.18	0.346	1.66	0.25	0.4	0.11	–	0.1400	0.0720	0.9264
	Tracer	6	25	1641	2.4	–	37.879	0.25	0.011	0.66	0.25	0.005	–	–	0.0183	0.0256	0.9973
	Uranium (VI)	6	25	1641	1.9	3.5	15.06	0.25	0.004	1.66	0.25	0.005	0.25	–	0.0924	0.0585	0.9810

L characteristic length [L]; v average pore-water velocity [LT^{-1}]; T_0 pulse duration [T]; R retardation factor; P Peclet number; β dimensionless variable for partitioning in nonequilibrium transport models (i.e., fraction of equilibrium sorption sites for two-site model and mobile water fraction for MIM model); ω dimensionless mass transfer coefficient; λ dispersivity [L]; θ_m/θ mobile water fraction; η transport parameter; f fraction of exchange sites assumed to be at equilibrium for the two-site model; fraction of adsorption sites that equilibrates with the mobile liquid phase for the two-region model; α first-order kinetic rate coefficient [T^{-1}]; *SSR* the sum of squares due to error; *RMSE* root mean squared error; R^2 coefficient of determination for curve fit to raw data

4.3 Nonequilibrium transport

Under unsaturated flow conditions, the equilibrium CDE was unable to accurately model the BTCs of either the tracer or the uranium, suggesting the occurrence of nonequilibrium behavior (Table 3, Fig. 3). Physicochemical processes that may induce nonequilibrium processes are the presence of simultaneously different adsorption kinetics and/or heterogeneous flow regime (Gamerdinger et al. 2001a, b). This occurrence of nonequilibrium transport is evident as we compare the BTCs of U(VI) to the BTCs of the conservative tracer under different pH conditions (Table 3, Fig. 3). In the CDE two-site model, the rate-limited sorption parameters β and ϖ were calculated to compute f and α (Table 3). In the CDE MIM model, the sorption is identical in the mobile and immobile water regions, and the sorption sites are distributed according to the distribution of mobile and immobile water regions.

The tracer BTCs do not indicate any chemical or physical nonequilibrium behavior. As the transport of U(VI) is well described by fitting it with nonequilibrium CDE models—two sites and MIM—it is tempting to conclude that the reactive transport of U(VI) in unsaturated porous media is subject to either a chemical nonequilibrium process (i.e., by different adsorption kinetics—either by instantaneous adsorption on one type of site or by first-order kinetics on the other type of site) or a physical nonequilibrium process (i.e., heterogeneous flow regime that can be simulated by two regions—a mobile water region and an immobile water region), or both concomitantly. Indeed, the modeling with nonequilibrium CDEs demonstrated that the asymmetry and shifts of the BTCs can be accurately depicted by these models (Table 3, Fig. 3). In the first approximation, one could assume that the reasonable fit of these models to experimental data indicates that the assumptions embodied in these models are legitimate. However, caution is in order since it is also entirely possible that these physical or chemical assumptions are misleading, and the reason the models fit the data well is that the models contain the right number of parameters, unlike the equilibrium model that falls short in that respect. Therefore, conclusions derived from model fitting exercises, even though it is interesting to analyze them to see where they lead, will have to be corroborated by microscopic evidence on the heterogeneity of sorption site, or on the true extent of partition of soil water into mobile and immobile phases.

Although the chemistry of the uranium solution (i.e., pH) has a direct impact on the occurrence of the chemical nonequilibrium process and related rate-limited mass transfer that govern U(VI) sorption and retention processes (i.e., decrease in sorption due to incomplete sorption), the decrease of availability of sorption sites as a result of MIM also impacts U(VI) sorption and retention processes. Gamerdinger et al. (2001b) have also reported that a decreased sorption may be due to "decreased availability of sorption sites induced by two-region flow at the lower water contents (<30 % saturation)."

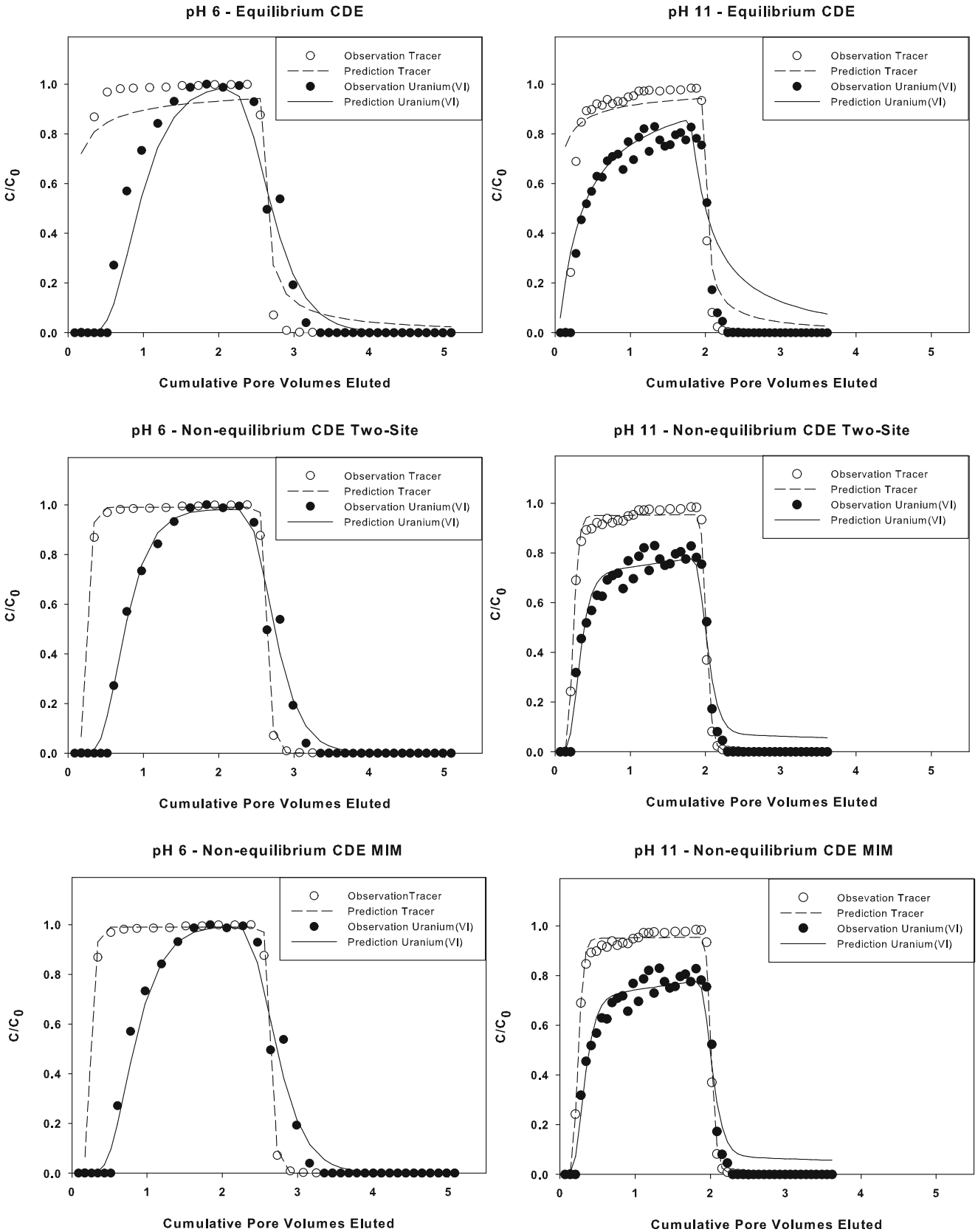

Fig. 3 Observed and predicted uranium(VI) transport in unsaturated sand at two pH values (pH 6 and 11). *Symbols* are the observed data and *lines* are the predictions modeled using equilibrium transport CDE and nonequilibrium transport CDE (two-site and MIM models)

Of particular interest is that at pH 6, the U(VI) BTC clearly exhibits a delay compared to the tracer. This finding may be the result of the two-site process dominating the sorption and retardation processes wherein MIM would contribute to a lesser degree. However, at pH 11, the U(VI) BTC is characterized by another delay that results in a BTC of a different shape compared to the one at pH 6. This result indicates that a different phenomenon may dominate the sorption and retardation processes. At pH 11, the hydraulic conditions of the unsaturated column are that the water velocity is higher and the water content is lower than at pH 6. The hydraulic conditions at pH 11 (<30 % saturation and fast water velocity) may decrease the sorption of U(VI) by decreasing the availability of sorption sites by inducing MIM, resulting then in MIM's being the dominant phenomenon in decreasing sorption sites compared to the role of the two-site process. Therefore, the CDE two-site model demonstrates the relationship between uranium adsorption and retardation during transport and rate-limited mass transfer processes, while the CDE MIM model establishes the critical influence of immobile water on the reactive transport of uranium.

5 Conclusions

Understanding the mobility of uranium in the vadose zone is critical to determining the potential contamination of nearby surface and groundwater resources. The coupled effects of unsaturated hydrodynamics and reactive transport of U(VI) affect the behavior of U(VI) in the vadose zone. The reactive transport of U(VI) governed by adsorption-desorption processes, precipitation and complexation reactions in which kinetic behaviors are controlled by pH and solution chemistry, and heterogeneous flow regime impact the mobility of U(VI) in the vadose zone. Near-neutral and alkaline pH values in the vadose zone waters generate different U(VI) behavior, including uranium speciation, uranium-harboring minerals, and dissolved uranium concentration, that result in significant differences in the fate and transport of U(VI). As the transport of U(VI) is well described by fitting it with nonequilibrium CDE models—two sites and MIM—we conclude tentatively that the reactive transport of U(VI) in unsaturated porous media is subject to the coupled effects of both a chemical nonequilibrium process (i.e., by different adsorption kinetics—either by instantaneous adsorption on one type of site or by first-order kinetics on the other type of site) and a physical nonequilibrium process (i.e., heterogeneous flow regime that can be simulated by two regions—a mobile water region and an immobile water region).

At pH 6 and under constant geochemical conditions, the transport of U(VI) is primarily controlled by adsorption processes as about 52 % of the added U(VI) adsorbed to the quartz sand. The U(VI) adsorption resulted in the retardation of U(VI). The desorption kinetics of U(VI) are significant, as observed through the elution of U(VI). Therefore, the fate of U(VI) in the vadose zone depends also on the reversibility of its adsorption that may occur following a change in geochemical conditions. The column transport experiments indicated that under specific geochemical conditions and vadose zone processes that favor the mobility of U(VI), dissolved- and colloidal-phase associations of U(VI) may be transported rapidly and at high concentration from the soil surface to the phreatic zone.

One interesting phenomenon captured by the adsorption/desorption processes of U(VI) to quartz sand is that variability in the geochemical solution conditions may give rise to significant U(VI) release in the vadose zone waters. This phenomenon may have implications for the roles of the vadose zone on the fate and transport of U(VI). The vadose zone may serve not only as a "transport pathway" of U(VI) between the soil surface and the water table, but it may also function as a "dynamic source" of U(VI), resulting in the persistent contamination of the phreatic zone. From this perspective, the episodic storage, release, and remobilization of U(VI) in the vadose zone appears highly dependent on the transient chemistry of the vadose zone waters causing changes in geochemistry and mineralogy, chemical reactions, and reaction kinetics, as well as on the transient infiltration processes under hydrological and climate changes.

Acknowledgments This research was supported by the U.S. Department of Energy, Office of Biological and Environmental Research, Environmental Remediation Sciences Program under grant number DE-FG02-06ER64193, and Clemson University. We thank Dr. Zhihong Xu, Editor-in-Chief of the *Journal of Soils and Sediments*, and the two anonymous reviewers for their thoughtful and constructive comments to improve our manuscript.

References

Abdelouas A, Lutze W, Nuttall E (1998) Chemical reactions of uranium in ground water at a mill tailings site. J Contam Hydrol 34:343–361

Aharoni C, Sparks DL (1991) Kinetics of soil chemical processes – A theoretical treatment. In: Sparks DL, Suarez DL (eds) Rate of soil chemical processes. Soil Sci Soc Am Spec Publ 27, Soil Sci Soc Am Inc, Madison, WI, pp 1–18

Andersson K, Torstenfelt B, Allard B (1982) Sorption behavior of long-lived radionuclides in igneous rock. In: International Atomic Energy Agency, the Commission of the European Communities and the OECD Nuclear Energy Agency (ed) Environmental migration of long-lived radionuclides, Vienna, Austria, pp 111–131

Arai Y, Marcus MK, Tamura N, Davis JA, Zachara JM (2007) Spectroscopic evidence for uranium bearing precipitates in vadose zone sediments at the Hanford 300-area site. Environ Sci Technol 41:4633–4639

Arnold T, Zorn T, Bernhard G, Nitsche H (1998) Sorption of uranium(VI) onto phyllite. Chem Geol 151:129–141

Arnold T, Zorn T, Zänker H, Bernhard G, Nitsche H (2001) Sorption behavior of U(VI) on phyllite: experiments and modeling. J Contam Hydrol 47:219–231

Artinger R, Rabung T, Kim JI, Sachs S, Schmeide K, Heise KH, Bernhard G, Nitsche H (2002) Humic colloid-borne migration of uranium in sand columns. J Contam Hydrol 58:1–12

Baik MH, Hahn PS (2001) Experimental study on uranium sorption onto silica colloids: effects of geochemical parameters. J Korean Nucl Soc 33:261–269

Ball MC, Brown DS, Perkins LJ (1997) Diffuse layers on the surface of mineral quartz. J Mater Chem 7:365–368

Bargar JR, Reitmeyer R, Lenhart JJ, Davis JA (2000) Characterization of U(VI)-carbonato ternary complexes on hematite: EXAFS and electrophoretic mobility measurements. Geochim Cosmochim Acta 64: 2737–2749

Barnett MO, Jardine PM, Brooks SC, Selim HM (2000) Adsorption and transport of uranium(VI) in subsurface media. Soil Sci Soc Am J 64: 908–917

Bethke CM (1996) Geochemical reaction modeling. Concepts and applications. Oxford University Press, New York

Bethke CM (2002) The Geochemist's Workbench® 4.0. University of Illinois, Urbana

Bickmore BR, Nagy KL, Young JS, Drexler JW (2001) Nitrate-cancrinite precipitation on quartz sand in simulated Hanford tank solutions. Environ Sci Technol 35:4481–4486

Bickmore BR, Nagy KL, Gray AK, Brinkerhoff AR (2006) The effect of Al(OH)4− on the dissolution rate of quartz. Geochim Cosmochim Acta 70:290–305

Cameron DA, Klute A (1977) Convective-dispersive solute transport with a combined equilibrium and kinetic adsorption model. Water Resour Res 19:718–724

Catalano JG, McKinley JP, Zachara JM, Heald SM, Smith SC, Brown GE (2006) Changes in uranium speciation through a depth sequence of contaminated Hanford sediments. Environ Sci Technol 40:2517–2524

Chen G, Flury M (2005) Retention of mineral colloids in unsaturated porous media as related to their surface properties. Colloids Surf A Physicochem Eng Asp 256:207–216

Cheng T, Barnett MO, Roden EE, Zhuang J (2007) Reactive transport of uranium(VI) and phosphate in a goethite-coated sand column: an experimental study. Chemosphere 68:1218–1223

Coats KH, Smith BD (1964) Dead-end pore volume and dispersion in porous media. Soc Petrol Eng J 4:73–84

Contardi JS, Turner DR, Ahn TM (2001) Modeling colloid transport for performance assessment. J Contam Hydrol 47:323–333

Crançon P, van der Lee J (2003) Speciation and mobility of uranium(VI) in humic-containing soils. Radiochim Acta 91:673–9

Crançon P, Pili E, Charlet L (2010) Uranium facilitated transport by water-dispersible colloids in field and soil columns. Sci Total Environ 408:2118–2128

CXTFIT/EXCEL (2013) CXTFIT code in excel. http://web.ornl.gov/~t6g/cxtfit/ (accessed 26 July 2014)

Fortner JA, Mertz CJ, Goldberg MM, Seifert S (2002) Characteristics of aqueous colloids generated by corrosion of metallic uranium fuel. ANL/CMT/CP-106586. Argonne National Laboratory, Argonne. http://www.ipd.anl.gov/anlpubs/2002/09/44366.pdf. Accessed 13 June 2013

Fox PM, Davis JA, Zachara JM (2006) The effect of calcium on aqueous uranium(VI) speciation and adsorption to ferrihydrite and quartz. Geochim Cosmochim Acta 70:1379–1387

Gabriel U, Gaudet J-P, Spadini L, Charlet L (1998) Reactive transport of uranyl in agoethite column: an experimental and modelling study. Chem Geol 151:107–128

Gamerdinger AP, Kaplan DI, Wellman DM, Serne RJ (2001a) Two-region flow and rate-limited sorption of uranium (VI) during transport in unsaturated silt loam. Water Resour Res 37:3147–3153

Gamerdinger AP, Kaplan DI, Wellman DM, Serne RJ (2001b) Two-region flow and decreased sorption of uranium (VI) during transport in Hanford groundwater and unsaturated sands. Water Resour Res 37:3155–3162

Giblin AM (1980) The role of clay adsorption in genesis of uranium ores. In: Ferguson J, Goleby AB (eds) Uranium in the Pine Creek geosyncline. International Atomic Energy Agency, Vienna, pp 521–529

Handley-Sidhu S, Bryan ND, Worsfold PJ, Vaughan DJ, Livens FR, Keith-Roach MJ (2009) Corrosion and transport of depleted uranium in sand-rich environments. Chemosphere 77:1434–1439

Ho CH, Miller NH (1986) Adsorption of uranyl species from bicarbonate solution onto hematite particles. J Colloid Interface Sci 110:165–171

Huber F, Lützenkirchen J (2009) Uranyl retention on quartz—new experimental data and blind prediction using an existing surface complexation model. Aquat Geochem 15:443–456

Jada A, Ait Akbour R, Douch J (2006) Surface charge and adsorption from water onto quartz sand of humic acid. Chemosphere 64:1287–1295

Jones TE, Wood MI, Corbin RA, Simpson BC (2001) Preliminary inventory estimates for single-shell tank leaks in B, BX, and BY tank farms. RPP-7389. CH2M Hill Hanford Group, Inc, Richland

Kaplan DI, Serne RJ (1995) Distribution coefficient values describing iodine, neptunium, selenium, technetium, and uranium sorption to Hanford sediments. PNL-10379, SUP. 1. Pacific Northwest Laboratory, Richland

Kaplan DI, Gervais TL, Krupka KM (1998) Uranium(VI) sorption to sediments under high pH and ionic strength conditions. Radiochim Acta 80:201–211

Ku TL, Luo S, Goldstein SJ, Murrell MT, Chu WL, Dobson PF (2009) Modeling non-steady state radioisotope transport in the vadose zone—a case study using uranium isotopes at Peña Blanca, Mexico. Geochim Cosmochim Acta 73:6052–6064

Larson LN, Stone JJ (2011) Sediment-bound arsenic and uranium within the Bowman-Haley Reservoir, North Dakota. Water Air Soil Pollut 219:27–42

Leduc LG, Ferroni GD, Trevors JT (1997) Resistance to heavy metals in different strains of Thiobacillus ferrooxidans. World J Microbiol Biotechnol 13:453–455

Lenhart JJ, Honeyman BD (1999) Uranium(VI) sorption to hematite in the presence of humic acid. Geochim Cosmochim Acta 63:2891–901

Lesher EK, Honeyman BD, Ranville JF (2013) Detection and characterization of uranium-humic complexes during 1D transport studies. Geochim Cosmochim Acta 109:127–142

Liu C, Zachara JM, Qafoku O, McKinley JP, Heald SM, Wang Z (2004) Dissolution of uranyl microprecipitates in subsurface sediments at Hanford site, USA. Geochim Cosmochim Acta 68:4519–4537

Liu CX, Zachara JM, Yantasee W, Majors PD, McKinley JP (2006) Microscopic reactive diffusion of uranium in the contaminated sediments at Hanford, United States. Water Resour Res 42:15

Liu C, Shi Z, Zachara JM (2009) Kinetics of uranium(VI) desorption from contaminated sediments: effect of geochemical conditions and model evaluation. Environ Sci Technol 43:6560–6566

Lu L, Conca J, Parker GR, Leonard PA, Moore B, Strietelmeier B, Triay IR (2000) Adsorption of actinides onto colloids as a function of time, temperature, ionic strength, and colloid concentration. Report LA-UR- 00-51-21. Los Alamos National Laboratory, Los Alamos

Ma R, Zheng C, Prommer H, Greskowiak J, Liu C, Zachara J, Rockhold M (2010) A field-scale reactive transport model for U(VI) migration influenced by coupled multirate mass transfer and surface complexation reactions. Water Resour Res. doi:10.1029/2009WR008168

Ma R, Zheng C, Liu C, Greskowiak J, Prommer H, Zachara J (2014a) Assessment of controlling processes for field-scale uranium reactive transport under highly transient flow conditions. Water Resour Res 50:1006–1024

Ma R, Liu C, Greskowiak J, Prommer H, Zachara J, Zheng C (2014b) Influence of calcite on uranium(VI) reactive transport in the groundwater-river mixing zone. J Contam Hydrol 156:27–37

Malin JN, Geiger FM (2010) Uranyl adsorption and speciation at the fused silica/water interface studied by resonantly enhanced second harmonic generation and the χ^3 method. J Phys Chem A 114:1797–1805

Mashal K, Harsh JB, Flury M, Felmy AR, Zhaq H (2004) Colloid formation in Hanford sediments reacted with simulated tank waste. Environ Sci Technol 38:5750–5756

McKinley JP, Zachara JM, Liu C, Heald SC, Prenitzer BI, Kempshall BW (2006) Microscale controls on the fate of contaminant uranium in the vadose zone, Hanford site, Washington. Geochim Cosmochim Acta 70:1873–1887

McKinley JP, Zachara JM, Wan J, McCready DE, Heald SM (2007a) Geochemical controls on contaminant uranium in vadose Hanford formation sediments at the 200 area and 300 area, Hanford site, Washington. Vadose Zone J 6:1004–1017

McKinley JP, Zachara JM, Smith SC, Liu C (2007b) Cation exchange reactions controlling desorption of $^{90}Sr^{2+}$ from coarse-grained contaminated sediments at the Hanford site, Washington. Geochim Cosmochim Acta 71:305–325

Mertz CJ, Fortner JA, Tsai Y (2003) Understanding the behavior and stability of some uranium mineral colloids. In: Finch RJ, Bullen DB (eds) Scientific basis for nuclear waste management XXVI, vol 757. Materials Research Society Symposium Proceedings, Warrendale, pp 489–496

Mibus J, Sachs S, Pfingsten W, Nebelung C, Bernhard G (2007) Migration of uranium(IV)/(VI) in the presence of humic acids in quartz sand: a laboratory column study. J Contam Hydrol 89:199–217

Mihalik J, Tlustos P, Szakova J (2011) The impact of an abandoned uranium mining area on the contamination of agricultural land in its surroundings. Water Air Soil Pollut 215:693–700

Miller AW, Rodriguez DR, Honeyman BD (2013a) Simplified behaviors from increased heterogeneity: I. 2-D uranium transport experiments at the decimeter scale. J Contam Hydrol 148:39–50

Miller AW, Rodriguez DR, Honeyman BD (2013b) Simplified behaviors from increased heterogeneity: II. 3-D uranium transport at the decimeter scale and intertank comparisons. J Contam Hydrol 148:51–66

Missana T, García-Gutiérrez M, Alonso Ú (2004) Kinetics and irreversibility of cesium and uranium sorption onto bentonite colloids in a deep granitic environment. Appl Clay Sci 26:137–150

Moyes LN, Parkman RH, Charnock JM, Vaughan DJ, Livens FR, Hughes CR, Braithwaite A (2000) Uranium uptake from aqueous solution by interaction with goethite, lepidocrocite, muscovite, and mackinawite: an X-ray absorption spectroscopy study. Environ Sci Technol 34:1062–1068

Nielsen DR, van Genuchten MT, Biggar JW (1986) Water flow and solute transport processes in the unsaturated zone. Water Resour Res 22: 89S–108S

Nkedi-Kizza P, Biggar JW, Selim HM, van Genuchten MT, Wierenga PJ, Davidson JM, Nielsen DR (1984) On the equivalence of two conceptual models for describing ion exchange during transport through an aggregated oxisol. Water Resour Res 20:1123–1130

Parker JC, van Genuchten MTh (1984) Determining transport parameters from laboratory and field tracer experiments. Bull 84–3, Va Agric Exp St, Blacksburg

Phillippi JM, Loganathan VA, McIndoe MJ, Barnett MO, Clement TP, Roden EE (2007) Theoretical solid/solution ratio effects on adsorption and transport: uranium(VI) and carbonate. Soil Sci Soc Am J 71:329–335

Prikryl JD, Jain A, Turner DR, Pabalan RT (2001) UraniumVI sorption behavior on silicate mineral mixtures. J Contam Hydrol 47:241–253

Qafoku NP, Ainsworth CC, Szecsody JE, Qafoku OS (2004) Transport-controlled kinetics of dissolution and precipitation in the sediments under alkaline and saline conditions. Geochim Cosmochim Acta 68: 2981–2995

Qafoku NP, Zachara JM, Liu C, Gassman PL, Qafoku OS, Smith SC (2005) Kinetic desorption and sorption of U(VI) during reactive transport in a contaminated Hanford sediment. Environ Sci Technol 39:3157–3165

Read D, Lawless TA, Sims RJ, Butter KR (1993) Uranium migration through intact sandstone cores. J Contam Hydrol 13:277–289

Redden G, Bargar J, Bencheikh-Latmani R (2001) Citrate enhanced uranyl adsorption on goethite: an EXAFS analysis. J Colloid Interface Sci 244:211–219

Reich T, Moll H, Arnold T, Denecke MA, Hennig C, Geipel G, Bernhard G, Nitsche H, Allen PG, Bucher JJ, Edelstein NM, Shuh DK (1998) An EXAFS study of uranium(VI) sorption onto silica gel and ferrihydrite. J Electron Spectrosc Relat Phenom 96:237–243

Rimstidt JD, Barnes HL (1980) The kinetics of silica-water reactions. Geochim Cosmochim Acta 44:1683–1699

Rod KA, Um W, Flury M (2010) Transport of strontium and cesium in simulated Hanford tank waste leachate through quartz sand under saturated and unsaturated flow. Environ Sci Technol 44: 8089–8094

Rod KA, Wellman DM, Flury M, Pierce EM, Harsh JB (2012) Diffuse release of uranium from contaminated sediments into capillary fringe pore water. J Contam Hydrol 140–141:164–172

Salter PF, Ames LL, McGarrah JE (1981) The sorption behavior of selected radionuclides on Columbia River basalts, RHO-BWI-LD-48. Rockwell Hanford Operations, Richland

Schnug E, Lottermoser BG (2013) Fertilizer-derived uranium and its threat to human health. Environ Sci Technol 47:2433–2434

Selim HM, Davidson JM, Mansell RS (1976) Evaluation of a two-site adsorption-desorption model for describing solute transport in soils. In Proc Summer Computer Simulation Conf, Washington, DC

Serne RJ, Clayton RE, Kutnyakov IV, Last GV, LeGore VL, Wilson TC, Schaef HT, O'Hara MJ, Wagnon KB, Lanigan DC, Brown CF, Williams BA, Lindenmeier CW, Orr RD, Burke DS, Ainsworth CC (2002) Characterization of vadose zone sediment: borehole 41-09-39 in the S-SX waste management area, PNNL-13757-3. U.S. Department of Energy, Pacific Northwest National Laboratory, Richland

Shang J, Liu C, Wang Z, Zachara JM (2011) Effect of grain size on uranium(VI) surface complexation kinetics and adsorption additivity. Environ Sci Technol 45:6025–6031

Shang J, Liu C, Wang Z, Zachara J (2014) Long-term kinetics of uranyl desorption from sediments under advective conditions. Water Resour Res 50:855–870

Sheppard MI, Thibault DH (1988) Migration of technetium, iodine, neptunium, and uranium in the peat of two minerotrophic mires. J Environ Qual 17:644–653

Sims R, Lawless TA, Alexander JL, Bennett DG, Read D (1996) Uranium migration through intact sandstone: effect of pollutant concentration and the reversibility of uptake. J Contam Hydrol 21:215–228

Stoliker DL, Kent DB, Zachara JM (2011) Quantifying differences in the impact of variable chemistry on equilibrium uranium(VI) adsorption properties of aquifer sediments. Environ Sci Technol 45:8733–8740

Stoliker DL, Liu C, Kent DB, Zachara JM (2013) Characterizing particle-scale equilibrium adsorption and kinetics of uranium(VI) desorption from U-contaminated sediments. Water Resour Res 49:1163–1177

Stubbs JE, Veblen LA, Elbert DC, Zachara JM, Davis JA, Veblen DR (2009) Newly recognized hosts for uranium in the Hanford Site vadose zone. Geochim Cosmochim Acta 73:1563–1576

Tang G, Mayes MA, Parker JC, Jardine PM (2010) CXTFIT/Excel—a modular adaptable code for parameter estimation, sensitivity analysis and uncertainty analysis for laboratory or field tracer experiments. Comput Geosci 36:1200–1209

Tompson AFB, Hudson GB, Smith DK, Hunt JR (2006) Analysis of radionuclide migration through a 200-m vadose zone following a 16-year infiltration event. Adv Water Resour 29:281–292

Toride N, Leij FJ, van Genuchten MT (1999) The CXTFIT code for estimating transport parameters from laboratory or field tracer experiments. Version 2.1, Research Report No. 137. U.S. Salinity Laboratory, U.S. Department of Agriculture, Riverside

Um W, Wang Z, Serne RJ, Williams BD, Brown CF, Dodge CJ, Francis AJ (2009) Uranium phases in contaminated sediments below Hanford's U tank farm. Environ Sci Technol 43:4280–4286

Um W, Icenhower JP, Brown CF, Serne RJ, Wang Z, Dodge CJ, Francis AJ (2010a) Characterization of uranium-contaminated sediments from beneath a nuclear waste storage tank from Hanford, Washington: implications for contaminant transport and fate. Geochim Cosmochim Acta 74:1363–1380

Um W, Zachara JM, Liu C, Moore DA, Rod KA (2010b) Resupply mechanism to a contaminated aquifer: a laboratory study of U(VI) desorption from capillary fringe sediments. Geochim Cosmochim Acta 74:5155–5170

US EPA (U.S. Environmental Protection Agency) (1999) Understanding variation in partition coefficient, Kd, values: volume II. Review of geochemistry and available Kd values for cadmium, cesium, chromium, lead, plutonium, radon, strontium, thorium, tritium (3H), and uranium. U.S. Environmental Protection Agency, Office of Air and Radiation. EPA 402-R-99-004B http://www.epa.gov/radiation/docs/kdreport/vol2/402-r-99-004b.pdf. Accessed 12 June 2013

van Genuchten MT, Wagenet RJ (1989) Two-site/two-region models for pesticide transport and degradation: theoretical development and analytical solutions. Soil Sci Soc Am J 53:1303–1310

van Genuchten MT, Wierenga PJ (1976) Mass transfer studies in sorbing porous media: I. Analytical solutions. Soil Sci Soc Am J 40:473–481

Viani BE, Torretto PC (1998) Sorption and transport of uranium on hematite. UCRL-ID-129848, YMP Milestone Report SPL3BM4 - 1997. Lawrence Livermore National Laboratory, Livermore

Waite TD, Davis JA, Payne TE, Waychunas GA, Xu N (1994) Uranium(VI) adsorption to ferrihydrite: application of a surface complexation model. Geochim Cosmochim Acta 58:5465–5478

Wang G, Um W (2012) Mineral dissolution and secondary precipitation on quartz sand in simulated Hanford tank solutions affecting subsurface porosity. J Hydrol 472–473:159–168

Wang Z, Zachara JM, Gassman PL, Liu C, Qafoku O, Yantasee W, Catalano JG (2005) Fluorescence spectroscopy of U(VI)-silicates and U(VI)-contaminated Hanford sediment. Geochim Cosmochim Acta 69:1391–1403

Wellman DM, Gamerdinger AP, Kaplan DI, Serne RJ (2008) Effect of particle-scale heterogeneity on uranium(VI) transport in unsaturated porous media. Vadose Zone J 7:67–78

Williams BA, Brown CF, Um W, Nimmons MJ, Peterson RE, Bjornstad BN, Lanigan DC, Serne RJ, Spane FA, Rockhold ML (2007) Limited field investigation report for uranium contamination in the 300 area, 300-FF-5 operable unit, Hanford Site, Washington. PNNL-16435. Pacific Northwest National Laboratory, Richland

Yabusaki SB, Fang Y, Waichler SR (2008) Building conceptual models of field-scale uranium reactive transport in a dynamic vadose zone-aquifer-river system. Water Resour Res. doi:10.1029/2007WR006617

Yabusaki SB, Fang Y, Williams KH, Murray CJ, Ward AL, Dayvault RD, Waichler SR, Newcomer DR, Spane FA, Long PE (2011) Variably saturated flow and multicomponent biogeochemical reactive transport modeling of a uranium bioremediation field experiment. J Contam Hydrol 126:271–290

Yin J, Haggerty R, Stoliker DL, Kent DB, Istok JD, Greskowiak J, Zachara JM (2011) Transient groundwater chemistry near a river: effects on U(VI) transport in laboratory column experiments. Water Resour Res. doi:10.1029/2010WR009369

Zachara JM, Ainsworth CC, McKinley JP, Murphy EM, Westall JC, Rao PSC (1992) Subsurface chemistry of organic ligand-radionuclide mixtures. In: Pacific Northwest Laboratory Annual Report for 1991 to the DOE Office of Energy Research Part 2: Environmental Science, PNL-8000 Pt. 2. Pacific Northwest Laboratory, Richland, pp 1–12

Zänker H, Hüttig G, Arnold T, Nitsche H (2006) Formation of iron-containing colloids by the weathering of phyllite. Aquat Geochem 12:299–325

Zheng Z, Wan J (2005) Release of contaminant U(VI) from soils. Radiochim Acta 93:211–217

Zhuang J, Flury M, Jin Y (2003) Colloid-facilitated Cs transport through water-saturated Hanford sediment and Ottawa sand. Environ Sci Technol 37:4905–4911

Zielinski RA (1980) Uranium in secondary silica: a possible exploration guide. Econ Geol 75:592–602